arXiv:1409.7550v1 [astro-ph.SR] 26 Sep 2014

Evidence of the Evolved Nature of the B[e] Star MWC 137 ⋆

M. F. Muratore [1]
Departamento de Espectroscopía Estelar, Facultad de Ciencias Astronómicas y Geofísicas, Universidad Nacional de La Plata, and Instituto de Astrofísica de La Plata, CCT La Plata, CONICET-UNLP, Paseo del Bosque S/N, B1900FWA, La Plata, Argentina
fmuratore@carina.fcaglp.unlp.edu.ar

M. Kraus and M. E. Oksala
Astronomický ústav, Akademie věd České Republiky, Fričova 298, 251 65 Ondřejov, Czech Republic

M. L. Arias [2] and L. Cidale [2]
Departamento de Espectroscopía Estelar, Facultad de Ciencias Astronómicas y Geofísicas, Universidad Nacional de La Plata, and Instituto de Astrofísica de La Plata, CCT La Plata, CONICET-UNLP, Paseo del Bosque S/N, B1900FWA, La Plata, Argentina

M. Borges Fernandes
Observatório Nacional, Rua General José Cristino 77, 20921-400 São Cristovão, Rio de Janeiro, Brazil
and

A. Liermann
Leibniz-Institut für Astrophysik Potsdam (AIP), An der Sternwarte 16, 14482 Potsdam, Germany

ABSTRACT

The evolutionary phase of B[e] stars is difficult to establish due to the un certainties in their fundamental parameters. For instance, possible classifications for the Galactic B[e] star MWC 137 include pre-main-sequence and post-main-sequence phases, with a large range in luminosity. Our goal is to clarify the evolutionary stage of this peculiar object, and to study the CO molecular component of its circumstellar medium. To this purpose, we modeled the CO molecular bands using high-resolution K-band spectra. We find that MWC 137 is surrounded by a detached cool ($T = 1900 \pm 100\,\mathrm{K}$) and dense ($N = (3 \pm 1) \times 10^{21}\,\mathrm{cm}^{-2}$) ring of CO gas orbiting the star with a rotational velocity, projected to the line of sight, of 84 ± 2 km s^{-1}. We also find that the molecular gas is enriched in the isotope ^{13}C, excluding the classification of the star as a Herbig Be. The observed isotopic abundance ratio ($^{12}\mathrm{C}/^{13}\mathrm{C} = 25 \pm 2$) derived from our modeling is compatible with a proto-PN, main-sequence or supergiant evolutionary phase. However, based on some observable characteristics of MWC 137, we propose that the supergiant scenario seems to be the most plausible. Hence, we suggest that MWC 137 could be in an extremely short-lived phase, evolving from a B[e] supergiant to a blue supergiant with a bipolar ring nebula.

Subject headings: Stars: early-type — Stars: emission-line, Be — circumstellar matter — Stars: individual (MWC 137)

1. INTRODUCTION

MWC 137 (V1380 Ori) is a peculiar early-type star located in the Galactic plane ($l = 195.65°, b = -0.07°$), surrounded by the optical nebula Sh 2-266 (PK 195-00°1). Its optical spectrum shows strong Balmer lines in emission, as well as permitted and forbidden emission lines from other elements, such as He I, Ca II, [O I], [O II], [N II], and [S II] (Hamann & Persson 1992; Zickgraf 2003; Hernández et al. 2004). This emission-line spectrum, together with the presence of a large infrared excess (Frogel et al. 1972; Cohen & Barlow 1975; Hillenbrand et al. 1992) usually attributed to free-free emission and thermal emission from dust, is responsible for the classification of this object as a B[e] star (Allen 1973; Bergner et al. 1995; Esteban & Fernández 1998; Marston & McCollum 2008).

Both the nature and evolutionary status of this object remain uncertain. Based on optical spectra and infrared photometry, Frogel et al. (1972) conclude that MWC 137 is probably an early-type emission-line star surrounded by nebulosity. Cohen & Barlow (1975) arrive to the same conclusion from the analysis of optical, infrared and radio data. Sabbadin & Hamzaoglu (1981) present photographic and spectroscopic observations, and propose that Sh 2-266 is likely a "low excitation nebula ejected and excited by a peculiar star". Due to the appearance of its emission-line spectrum, this star has been included in many catalogs and articles on Herbig Ae/Be stars (Hillenbrand et al. 1992; Berrilli et al. 1992; Thé et al. 1994). Based on photometric and spectroscopic studies, Miroshnichenko (1994) and Bergner et al. (1995) conclude that this object is an early-B type star near the zero-age main sequence (ZAMS), although the latter state that it is not clear whether it is a pre-main-sequence object, or a more massive star that has just left the main sequence. Some authors, however, argue against a pre-main-sequence nature of the object based on its high luminosity, the shape of the Hα, Na I D and He I 5876 Å line profiles, and the fact that the radio emission at 10 GHz is much stronger than in any other Herbig Be star (Herbig & Kameswara Rao 1972; Finkenzeller & Mundt 1984). On the other hand, Manchado et al. (1989) classify the star as a late B-type supergiant based on a photometric analysis, while Esteban & Fernández (1998), using high-resolution spectroscopy and Hα imaging, conclude that the star is an evolved early B supergiant. While most studies agree on assigning an early spectral type to the star, ranging from late O (Brand & Wouterloot 1994; Rudolph et al. 1996) to early B (Hillenbrand 1995; Miroshnichenko 1994), the determination of the luminosity class is still subject to debate. This is due to the fact that few photospheric absorption features are seen in the stellar spectrum. In addition, the amount of circumstellar extinction is not known, complicating the distance and luminosity determination.

The nebula around MWC 137 was first classified as an H II region by Sharpless (1959), who designated it as Sh 2-266. Values for the kinematical distance, obtained under the assumption that the H II region was associated with a molecular cloud with measured CO velocity, include: 12.6 ± 3.2 kpc (Fich & Blitz 1984; Wouterloot et al. 1988), 9.6 ± 4.8 kpc (Fich & Silkey 1991), and 10.98 kpc (Brand & Wouterloot 1994). This object was also cataloged as the planetary nebula (PN) PK 195-00°1 by Perek & Kohoutek (1967), and although subsequent work questioned this classification (Frogel et al. 1972; Cohen & Barlow 1975), it continued to appear in many PNe studies. Distances derived with methods developed specifically for PNe range from 870 pc (Amnuel et al. 1984) to 1.62 kpc (Zhang 1995). Herbig Be studies usually adopt distances of the order of 1 kpc, leading to luminosities in the range $\log(L/L_\odot) \sim 4.2-4.5$ (e.g. Hillenbrand et al. 1992). Esteban & Fernández (1998) use high-resolution spectroscopy to measure the radial velocity of different nebular lines, and derive a kinematical distance $d \geq 6$ kpc. With this lower limit for the distance, the authors ob-

* Based on observations obtained at the Gemini Observatory, which is operated by the Association of Universities for Research in Astronomy, Inc., under a cooperative agreement with the NSF on behalf of the Gemini partnership: the National Science Foundation (United States), the National Research Council (Canada), CONICYT (Chile), the Australian Research Council (Australia), Ministério da Ciência, Tecnologia e Inovação (Brazil) and Ministerio de Ciencia, Tecnología e Innovación Productiva (Argentina), under program IDs GN-2011B-Q-24 and GN-2013B-Q-11.

[1] Research Fellow of the Universidad Nacional de La Plata, Argentina

[2] Member of the Carrera del Investigador Científico, CONICET, Argentina

tain a luminosity $\log(L/L_{\odot}) \geq 5.4$, compatible with a supergiant evolutionary stage.

A way to disentangle the nature of MWC 137 (and of unclassified B[e] stars in general) is to analize the properties of the circumstellar material (spatial distribution, composition, physical conditions, and kinematics), since they are directly related to the evolutionary stage of the underlying object. The first overtone CO band emission visible in the K band constitutes an extremely valuable tool for obtaining information about the star and the surrounding material. This feature has been observed in a variety of objects, including pre-main-sequence (e.g. Carr 1995; Najita et al. 1996) and evolved stars, both low-mass (e.g. Gorlova et al. 2006; Gledhill et al. 2011) and high-mass (e.g. McGregor et al. 1988a,b; Morris et al. 1996; Oksala et al. 2013). It originates in the inner edge of a molecular circumstellar disk, making it an ideal indicator for both the disk parameters (temperature and density) and kinematics. In addition, the chemical composition of the molecular material around evolved stars can provide information about the evolutionary stage of the star at the time of mass ejection.

During the evolution of stars, heavy elements produced in the stellar interior are transported to the surface via rotation and mixing processes. Since the stellar surface abundance of ^{13}C increases with the age of the star (Kraus 2009), this element is a very valuable tracer for stellar evolution. Mass loss deposits the chemically enriched matter into the circumstellar environment, where it condenses into molecules. The detection of ^{13}CO emission bands with high-resolution spectrographs reflects the existence of a substantial amount of ^{13}C in the circumstellar medium (Kraus 2009). The idea of using ^{13}CO as an indicator of the stellar evolutionary phase was proposed by Kraus (2009), and applied by Liermann et al. (2010), Muratore et al. (2010), Kraus et al. (2013), and Oksala et al. (2013), to confirm the evolved nature of several objects, including B[e] supergiants and yellow hypergiants. This method is extremely useful for stars with ambiguous classification, such as MWC 137, because it allows to distinguish evolved stars from young, pre-main-sequence objects.

In this work we investigate the CO emission from MWC 137 using high-resolution near-infrared spectroscopy. The presence of ^{12}CO band emission was reported by Muratore et al. (2012) and Oksala et al. (2013). In addition, Oksala et al. (2013) detected ^{13}CO emission bands, which were confirmed by Liermann et al. (2014). Based on the amount of ^{13}CO present in the K-band spectrum, these authors suggest that the star is not a pre-main-sequence object. Given that their result was based on low-resolution data, it is important to confirm the ^{13}C enrichment, since it could constrain the evolutionary state of the star. In addition, it could also provide evidence about the origin of the CO disk and gaseous nebula (accreted vs ejected material). When the disk is formed of material ejected by a hot massive star, the presence of molecules and dust within a few tens of AU from the star is not expected due to the high UV radiation flux. Therefore, it is crucial to investigate the physical and kinematical properties of such circumstellar envelopes, since the formation and survival of dust and molecules under harsh conditions is one of the unresolved issues of stellar evolution. Furthermore, it is important to know the amount of mass ejected by the star in previous stages of the evolution, since it could affect the properties of the object in the following phases (e.g., evolution time-scale, fate of the star).

2. OBSERVATIONS

High resolution ($R \sim 18000$) K-band spectroscopic observations of MWC 137 were obtained in 2011 and 2014 using the Gemini Near-Infrared Spectrograph (GNIRS) mounted on the Gemini North telescope. The observations taken in 2011, which included the first two ^{12}CO band heads, were aimed at studying the kinematics and physical properties of the gas. The goal of the second set of observations, obtained in 2014, was to confirm the presence of ^{13}CO emission and model it in detail. The spectral range covered by the 2011 GNIRS observations was also included to check the possible variability of the ^{12}CO bands. Details related to the observing programs can be found in Table 1. The observations were performed in longslit mode, using the long camera, the 110 l/mm grating, and the 0.10 arcsec slit. A central wavelength of 2.312 μm was chosen in 2011, while two wavelength intervals, centered at 2.312 and 2.36 μm, were observed in 2014. Observations were taken with an ABBA nod pattern along the

Table 1: Details on MWC 137 K-band observations.

Program ID	Instrument	Date	Spectral Range (μm)	CO Coverage
GN-2011B-Q-24	GNIRS	2011-10-07	$2.28 - 2.34$	first two ^{12}CO band heads
GN-2013B-Q-11	GNIRS	2014-03-21	$2.28 - 2.39$	four ^{12}CO band heads, first two ^{13}CO band heads

slit in order to remove sky emission. All the steps of the reduction process were made using IRAF[1] software package tasks. Reduction steps include AB pairs subtraction, flat field correction, telluric correction, and wavelength calibration. The telluric correction was performed using a B-type telluric standard star observed at similar airmass. After applying the corrections for heliocentric and systemic velocities, the continuum was used to normalize the data, and finally, it was subtracted to obtain pure emission spectra.

Fig. 1 shows the normalized, continuum-subtracted GNIRS spectra from 2011 (bottom panel) and 2014 (top panel), which clearly display the CO first overtone bands in emission. In addition, the spectrum from 2014 shows emission lines from the hydrogen Pfund series superimposed on the molecular bands. These lines are also present in the 2011 spectrum, but they are not so easily distinguished in this spectral range. The ticks in the figure mark the position of the ^{12}CO and ^{13}CO band heads, and the wavelengths corresponding to the Pfund transitions. Both spectra look similar, which implies that the CO emission has not changed significantly in the last two years.

3. SPECTRAL MODELING

The physical conditions and kinematics of the CO emitting region can be determined by modeling the emission bands present in our K-band spectra of MWC 137. However, the amount of ^{13}CO present in the circumstellar environment can only be determined by modeling the spectrum obtained in 2014. Given that the CO emission did not change significantly between the two epochs, in this section we describe in detail the modeling and the results obtained from the 2014 spectrum, since its spectral coverage allows to study both, the ^{12}CO and the ^{13}CO band emission. The contribution of the Pfund lines to the observed spectrum must also be taken into account to properly fit the CO band emission. At the end of this section we compare the results obtained from fitting the spectra taken in both epochs to check for possible differences.

3.1. Description of the Models

The Pfund emission lines do not appear to be double-peaked, hence they do not originate in a rotating disk, but most probably in a high-density ionized wind or shell. We use the code developed by Kraus et al. (2000), which, following Menzel's recombination theory (Baker & Menzel 1938), computes the emission from these lines under the assumption that they are optically thin. The line profiles are assumed to have a Gaussian shape, characterized by the velocity $v_{\rm gauss,Pf}$. The physical properties of the gas are given by the electron density n_e, the proton density n_p, which for simplicity we set equal to n_e, and the electron temperature T_e. Since the population of the higher levels can be prevented by pressure ionization effects in high-density media, the code allows to specify the quantum number $\rm n_{max}$ of the maximum transition included in the computation. This will be used to determine a lower limit for $n_e = n_p$.

The shape of the first ^{12}CO band head gives an indication of the kinematical broadening of the individual CO lines. Fig. 2 shows a blowup of the GNIRS spectrum in the region of the first ^{12}CO band head. The blue shoulder and the red peak are both characteristic of emission originated in a rotating ring of material (e.g. Carr et al. 1993; Carr 1995; Najita et al. 1996; Kraus et al. 2000). We model the CO bands using the ^{12}CO disk code of Kraus et al. (2000), modified to include ^{13}CO (Kraus 2009; Oksala et al. 2013). This code com-

[1]IRAF is distributed by the National Optical Astronomy Observatories, which are operated by the Association of Universities for Research in Astronomy, Inc., under cooperative agreement with the National Science Foundation.

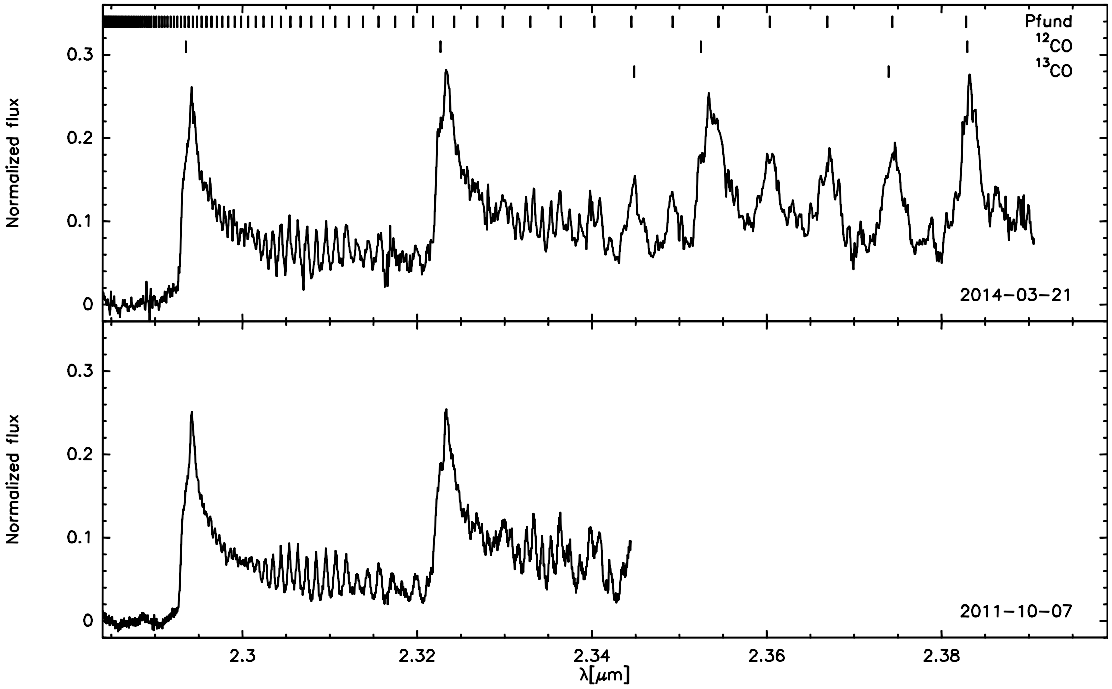

Fig. 1.— Normalized, continuum-subtracted GNIRS spectra from 2011 (bottom panel) and 2014 (top panel). The position of the ^{12}CO and ^{13}CO band heads, and the wavelengths corresponding to the Pfund transitions are indicated.

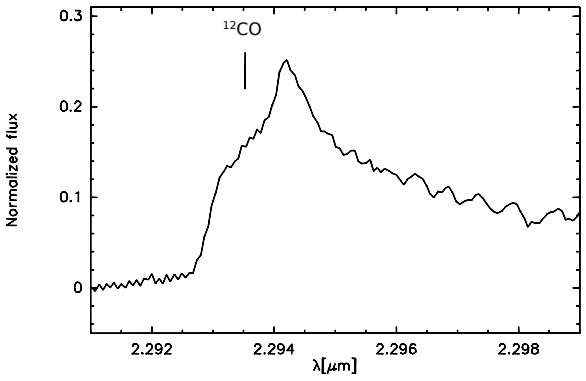

Fig. 2.— Normalized, continuum-subtracted GNIRS spectrum showing in detail the rotationally broadened structure of the first ^{12}CO band head. The tick marks the position of the band head.

putes the ^{12}CO and ^{13}CO emission arising from a narrow ring of material with constant temperature $T_{\rm CO}$, column density $N_{\rm CO}$, rotational velocity projected to the line of sight $v_{\rm rot,CO}\sin i$, and a given isotopic abundance ratio ^{12}C/^{13}C. These choices reflect the fact that the CO emission is usually found to arise from a disk, and that the hottest component, assumed to be located in a relatively narrow region, is mainly responsible for the observed CO spectrum (Kraus et al. 2000; Kraus 2009; Liermann et al. 2010; Cidale et al. 2012; Kraus et al. 2013).

To derive the characteristics of the CO emitting region, we model simultaneously the contribution to the K-band spectrum of both the CO band emission and the Pfund line emission.

3.2. Results

The width and shape of the Pfund lines are well fit by a Gaussian profile with $v_{\rm gauss,Pf} = 170 \pm 10$ km s^{-1}. Since the separation between the individual lines decreases as the transitions become higher, the Pfund lines start to blend towards

shorter wavelengths and form a quasi-continuum. The wavelength where this occurs depends on the width of the lines and the resolution of the spectrum. Taking into account the broad profiles of the Pfund lines and the resolution of the GNIRS spectrum, this quasi-continuum should start at $\lambda < 2.32\,\mu$m, and extend down to the Pfund discontinuity at $\lambda \sim 2.28\,\mu$m. However, we find from the modeling that the contribution of the Pfund series is limited to a certain number of transitions, being Pf(55) the maximum transition present. The fact that the cut off occurs at such a low transition indicates a very high electron density. The lowest value of the density compatible with $n_{max} = 55$ can be estimated by considering pressure ionization effects, which gives $n_e > 10^{12}$ cm^{-3} (Kraus 2000). The Pfund lines visible in the GNIRS spectrum correspond to transitions associated with quantum numbers in the range 24 - 55. Given the high electron density, the deviation from LTE is negligible for these members of the series (see Kraus 2000). Furthermore, the relative intensities of these lines are not sensitive to the electron temperature, so we modeled the final Pfund spectrum with $n_e = 10^{13}$ cm^{-3} and a fixed electron temperature $T_e = 10\,000$ K, representative of an ionized nebula.

The kinematics of the CO gas can be easily extracted from the shape of the first band head. Fig. 2 shows the rotationally broadened structure, and modeling yields a rotational velocity, projected to the line of sight, of $v_{\rm rot,CO} \sin i = 84 \pm 2$ km s^{-1}. The structure of the ^{12}CO bands is sensitive to the temperature and column density of the gas in the emitting region, as described in Kraus (2000, 2009). Due to the high resolution of the GNIRS spectrum, the temperature can be determined from the appearance of the features in the region in front of the second band head. This results in a value of $T_{\rm CO} = 1900 \pm 100$ K. Determination of the column density requires a wider spectral range than the one used to derive the temperature. From the modeling of the four CO band heads visible in the last spectrum taken with GNIRS we obtain $N_{\rm CO} = (3\pm1)\times10^{21}$ cm^{-2}. Considering that the dissociation temperature for the CO molecule is $\sim$ 5000 K, the derived temperature implies that the material producing the band head structure is rather cool, suggesting it is detached from the star.

With fixed values for temperature, column density, and rotational velocity, we first compute the CO emission spectrum with a carbon isotopic abundance ratio ^{12}C/^{13}C = 90. According to stellar evolution models, this value corresponds approximately to the beginning of the main sequence (see, e.g., Ekström et al. 2012). The top panel of Fig. 3 shows the resulting Pfund + CO model (red solid line) superimposed on the observed emission spectrum (black solid line). The pure Pfund emission model is also included in this plot (blue dotted line). The ticks mark the wavelengths corresponding to the Pfund transitions and the position of the ^{13}CO band heads. A closer inspection of the fit shows that some flux appears to be missing redward of $\lambda \sim 2.34\,\mu$m. Models with lower and higher column densities are not able to reproduce the continuum level and/or the intensity of the band heads. Thus, the only way to improve the fit is to increase the contribution of ^{13}CO, or in other words, lower the isotopic abundance ratio. The best fit is obtained for a value ^{12}C/^{13}C $= 25 \pm 2$. The middle panel of Fig. 3 shows this model (red solid line) together with the GNIRS spectrum (black solid line). Comparison between both fits clearly shows that the isotope ^{13}CO contributes to the K-band emission. To help visualize the difference between the models in the regions of the ^{13}CO band heads, a plot showing the residuals of the fits was included in the bottom panel. The dotted curve corresponds to the residual of the fit for the model with ^{12}C/^{13}C = 90 (i.e., without ^{13}CO), and the solid line represents the residual of the fit for the model with ^{12}C/^{13}C = 25 (i.e., with ^{13}CO). The "crosses" mark the wavelength and FWHM of the two ^{13}CO band head structures. The complete set of derived Pfund and CO parameters is listed in Table 2.

The variation of the ^{12}C and ^{13}C surface abundances predicted by the stellar evolution models of Ekström et al. (2012) implies that the surface ratio ^{12}C/^{13}C drops from an initial value of ~ 90 to less than $\sim 20 - 30$ by the end of the main sequence, depending on the initial mass of the star. The value of 25 ± 2 obtained for MWC 137 confirms earlier suggestions by Oksala et al. (2013), who obtained a tentative value of 25 ± 5 based on a low-resolution spectrum. This indicates that the star is definitively not a pre-main-sequence object, validation that the Herbig Be classification

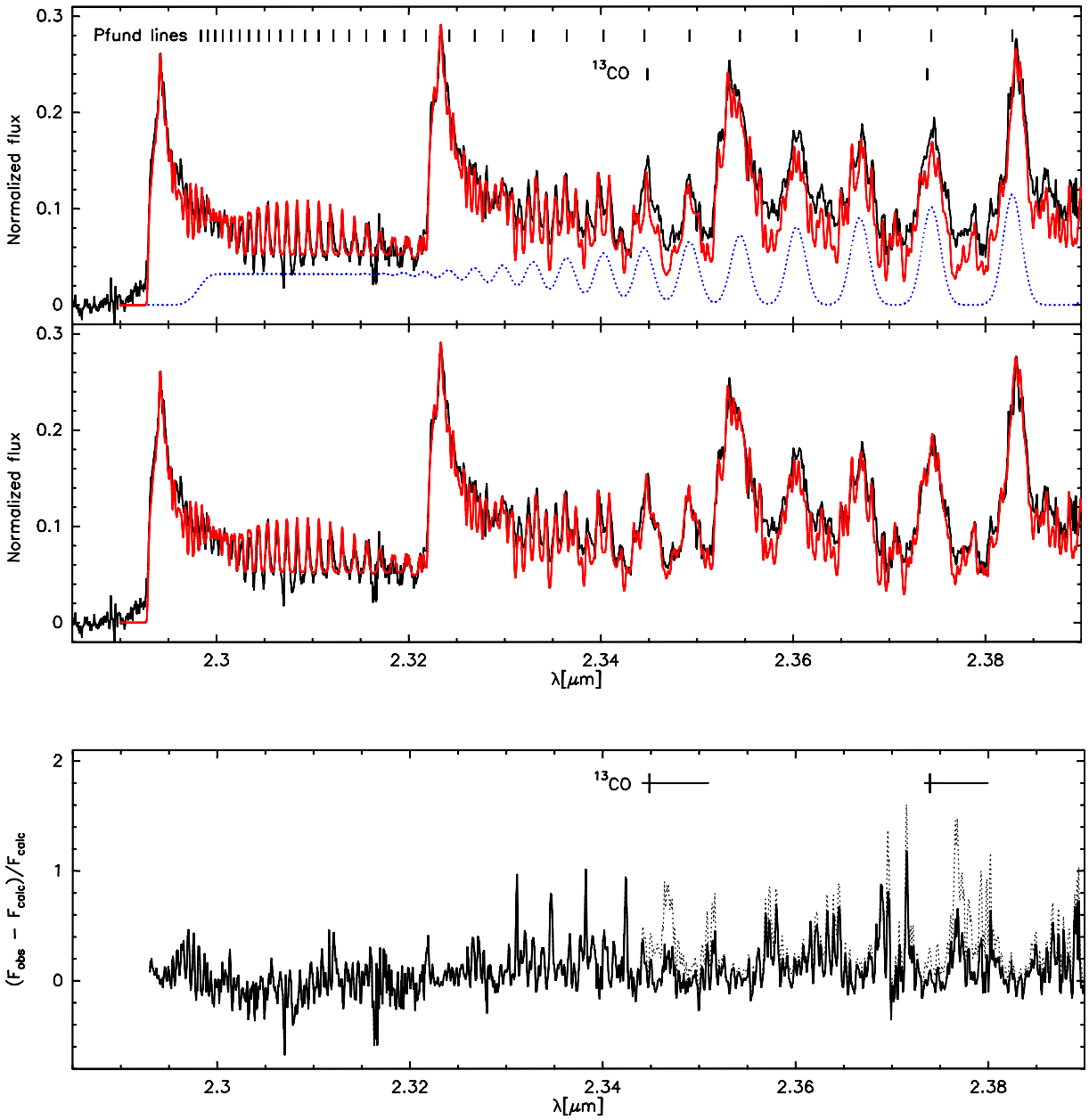

Fig. 3.— *Top and middle panels:* Normalized, continuum-subtracted GNIRS spectrum (black) along with the best-fit models (red) obtained for the combined Pfund + CO emission assuming a ratio of $^{12}C/^{13}C = 90$ (top) and $^{12}C/^{13}C = 25$ (middle). The synthetic Pfund emission spectrum (blue dotted line) included in the models is shown separately in the top panel. The position of the Pfund transitions and the ^{13}CO band heads is also indicated. *Bottom panel:* Residuals of the fits for the models with $^{12}C/^{13}C = 90$ (dotted black line) and $^{12}C/^{13}C = 25$ (black solid line). The "crosses" mark the wavelength and FWHM of the two ^{13}CO band head structures.

can finally be discarded. This important result still holds when other stellar evolution models are considered, since the initial value and the variation of the carbon isotopic ratio along stellar evolution are similar in all of them (see, e.g., the tracks from Brott et al. 2011; Chieffi & Limongi 2013).

It is worth mentioning that the CO parameters obtained from the fits to the 2011 and 2014 spectra are the same. However, an increase in the contribution of the Pfund emission between these two epochs was found. The top panel of Fig. 4 shows the best-fit CO + Pfund model (red solid line) superimposed on the spectra (black solid line) taken in 2014. The same fit is overplotted in the bottom panel to the spectrum taken in 2011. Obviously, the shape of the observed spectrum is the same as in 2014, but the fit redward of $\sim 2.3\,\mu$m overestimates the global intensity. To reduce the flux in this region, we found that a reduction in the contribution of the Pfund emission (dashed line versus dotted line) is necessary, while the CO model remains unaltered. The difference in these Pfund contributions might indicate a slight increase in the wind emission between the two epochs, although the cause of this variability is not so clear. On the other hand, the shape and intensity of the CO emission bands do not appear to have changed, which might point to a certain stability of the disk or ring structure where they originate. This kind of stability is usually associated with Keplerian rotation, but more observations are needed to confirm the non-variable character of the CO emission.

4. DISCUSSION

From the ^{13}C enrichment of the circumstellar material detected in the K-band spectrum, it is clear that MWC 137 cannot be a pre-main-sequence object. Considering the other classifications reported by different authors and the variation of the ^{12}C/^{13}C ratio along the stellar evolution, in this section we analyze which evolutionary scenarios are compatible with the value of the isotopic abundance ratio derived from our modeling. After giving a quick overview of some of the differences and similarities between MWC 137 and objects in each of these evolutionary phases, we briefly discuss whether it is possible to constrain the evolutionary stage of this star even further based on the results of our data.

Table 2: Best fit model parameters.

$v_{\rm gauss,Pf}$	170 ± 10 km s^{-1}
$\rm n_{max}$	55
n_e	10^{13} cm^{-3}
T_e	10 000 K
$v_{\rm rot,CO} \sin i$	84 ± 2 km s^{-1}
$T_{\rm CO}$	1900 ± 100 K
$N_{\rm CO}$	$(3 \pm 1) \times 10^{21}$ cm^{-2}
^{12}C/^{13}C	25 ± 2

Although the classifications found in the literature are based on assumptions of different nature, their plausibility depends strongly on the distance to the object, which is still uncertain. Unfortunately, our data cannot support neither confirm the distances previously estimated. Even though some distance estimates found in the literature might be more reliable than others, such a discussion is out of the scope of this work. Thus, our discussion will only be based on the value of the carbon isotopic ratio.

4.1. ^{12}C/^{13}C Ratio and Stellar Evolution

Table 3 lists effective temperature and luminosity determinations taken from the literature. The classification and distance assumed by the different authors are also included. Fig. 5 shows the location of the star in the HR diagram based on these determinations together with the evolutionary tracks from Ekström et al. (2012) for non-rotating (left panel) and rotating (right panel) stars of solar metallicity. The rotating evolutionary tracks were computed for an initial rotation rate $v_{\rm ini}/v_{\rm crit} = 0.40$. The accuracy of these well-known stellar evolution models is enough for our purpose, since the uncertainty in the stellar parameters is by far larger than the difference between evolutionary tracks from different authors (a comparison between stellar evolution models can be found in Martins & Palacios 2013). From the tables provided by Ekström et al. (2012) we compute the ^{12}C/^{13}C ratio along the stellar evolution, and indicate in the figures those parts of the tracks (solid blue line) that are compatible with the ratio of 25 ± 2 derived for MWC 137.

Taking into account the classifications listed in Table 3, all the positions of the star in the HR

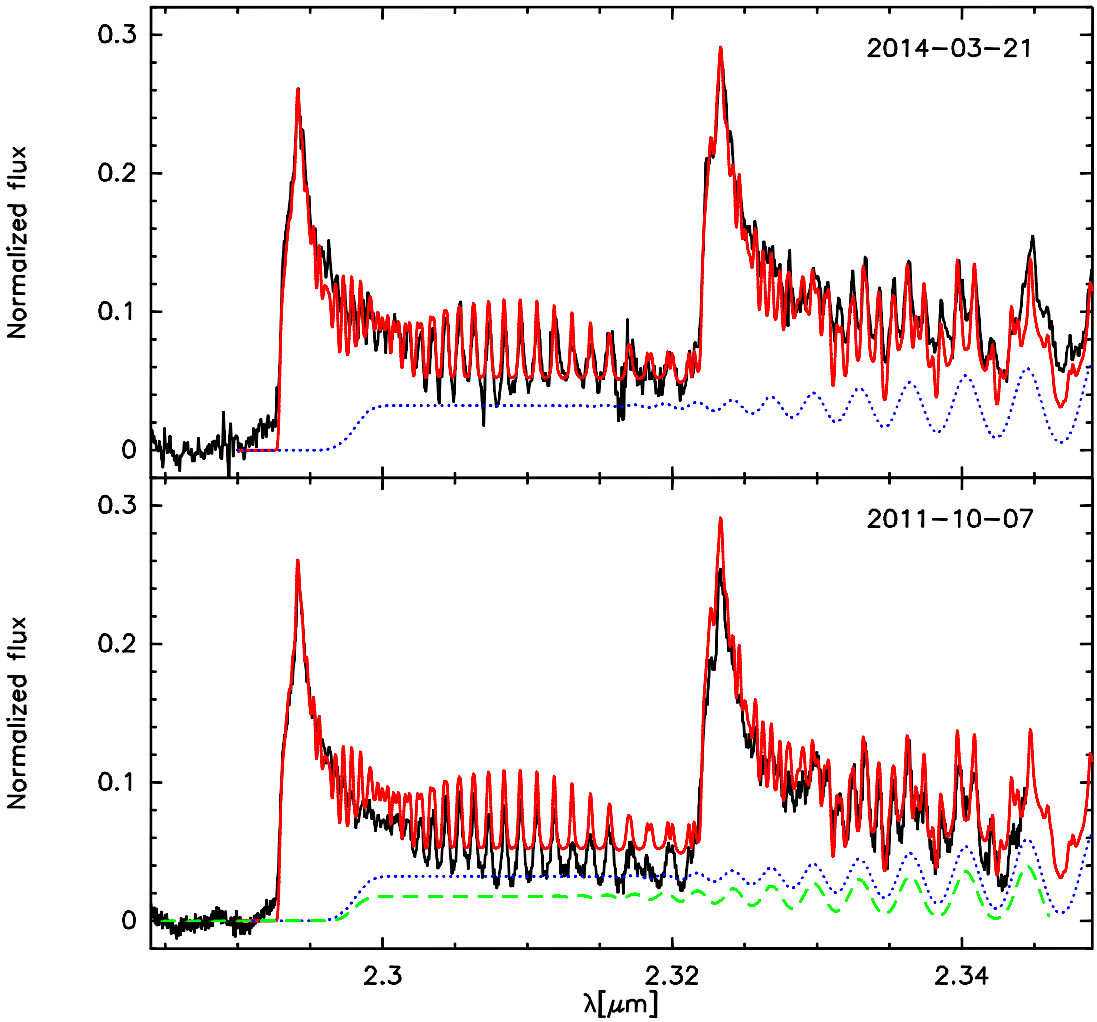

Fig. 4.— Normalized, continuum-subtracted GNIRS spectrum from 2014 (top panel, black solid line) along with the best-fit CO + Pfund model (red solid line). The contribution of the Pfund emission is shown in blue dotted line. The best-fit to the 2014 spectrum is shown in the bottom panel superimposed on the 2011 spectrum. The contribution of the Pfund emission to the 2011 and 2014 spectra are shown in green dashed and blue dotted lines, respectively.

diagram correspond to ratios higher than 30 for the non-rotating case, as can be seen in the left panel of Fig. 5. This is clearly inconsistent with the value of 25 ± 2 obtained from our fit. The right panel of this figure shows that the lower luminosity positions are compatible with a main-sequence star of initial mass between 12 and 16 $M_\odot$, and initial rotation rate similar to the value used to compute the stellar evolution models. The higher luminosity position could correspond to a supergiant star of initial mass of at least 25 - 32 $M_\odot$, but with a lower initial rotation rate than the one that was used to compute these tracks. The possibility of the star being in the PN phase cannot be analyzed in the same way because there are no determinations of effective temperature or luminosity made under that assumption. However, if we consider the position in the HR diagram corresponding to the lowest luminosity, we find that it could be compatible with a star of initial mass around 9 $M_\odot$, with a very low initial rotation rate, that expelled the enriched material in a previous phase (AGB and post-AGB) and is now evolving towards the PN phase. In the following section we analyze each of these possibilities and their implications.

4.2. Possible Scenarios

4.2.1. Planetary Nebula

The luminosity corresponding to the lowest position in the HR diagram, $\log(L/L_\odot) = 4.18$, is relatively high for PNe but still compatible with this class of objects (see evolutionary tracks from, e.g., Paczyński 1970, 1971; Vassiliadis & Wood 1994; Blöcker 1995). Contrary to what is expected for typical PNe, the [O III] emission in MWC 137 is very weak (Frogel et al. 1972; Sabbadin & Hamzaoglu 1981). However, Kraus et al. (2005) found that the [O III] emission from the PN Hen 2-90 is not as strong as expected for normal PNe, and explain this with a very low O abundance. Another possibility is that the temperature of the star is not yet high enough to ionize O II. Central stars of PNe with such low temperatures might be at the (early) beginning of the PN phase, so in other words, they might be young PNe. However, these stars are often considered to be "transition objects" evolving from the AGB to the PN phase, and they are referred to as pre- or proto-PNe. One of the best studied proto-PNe, M 1-92 (Minkowski's Footprint) was also reported to show very weak [O III] emission (Bujarrabal et al. 1998b). Furthermore, the sizes of the nebulae around this object and MWC 137 are comparable, with a total extension of 0.2 pc (Bujarrabal et al. 1998a) and 0.3 pc, respectively. The latter was estimated considering an angular diameter of $\sim 1'$, and a distance of ~ 1 kpc, which is the average value corresponding to the PN scenario. One of the characteristics usually associated with proto-PNe and PNe is the presence of H_2 emission in the near infrared. García-Hernández et al. (2002) and Kelly & Hrivnak (2005) found that almost all the B-type stars in their proto-PNe samples showed emission from the 2.122 μm H_2 line, with the exception of one object in each sample. Furthermore, Kelly & Hrivnak (2005) found that all the B stars that showed H_2 emission also presented Brγ emission, although in most cases this line was weaker than the 2.122 μm line. MWC 137 exhibits the Brγ line in strong emission, but no H_2 lines have been detected (Oksala et al. 2013), which might suggest that the star is not in a proto-PN phase. However, García-Hernández et al. (2002) and Kelly & Hrivnak (2005) proposed several explanations for the lack of detection of H_2 emission in the B-type stars included in their samples (e.g., misplacement of the slit, weak emission due to photodissociation), so this scenario cannot be ruled out yet.

Near-infrared CO band emission has been detected in the spectra of post-AGB stars (e.g. Hrivnak et al. 1994; García-Hernández et al. 2002; Oudmaijer et al. 1995; Gledhill et al. 2011) and proto-PNe (Hora et al. 1999), indicating that this molecule can be present in the circumstellar environment of these objects. Compact molecular disks have been detected around post-AGB stars and proto-PNe, and although the material is usually found to be in expansion, rotation has been proposed in several cases, and confirmed at least in one object, the proto-PN HD 44179, known as the Red Rectangle nebula (Bujarrabal & Alcolea 2013). The low luminosity position of MWC 137 in the HR diagram and the derived value of the carbon isotopic ratio are compatible with a PN stage only for a very low initial rotation rate. If the CO band emission observed in the spectrum of MWC 137 comes from a rotating ring with a veloc-

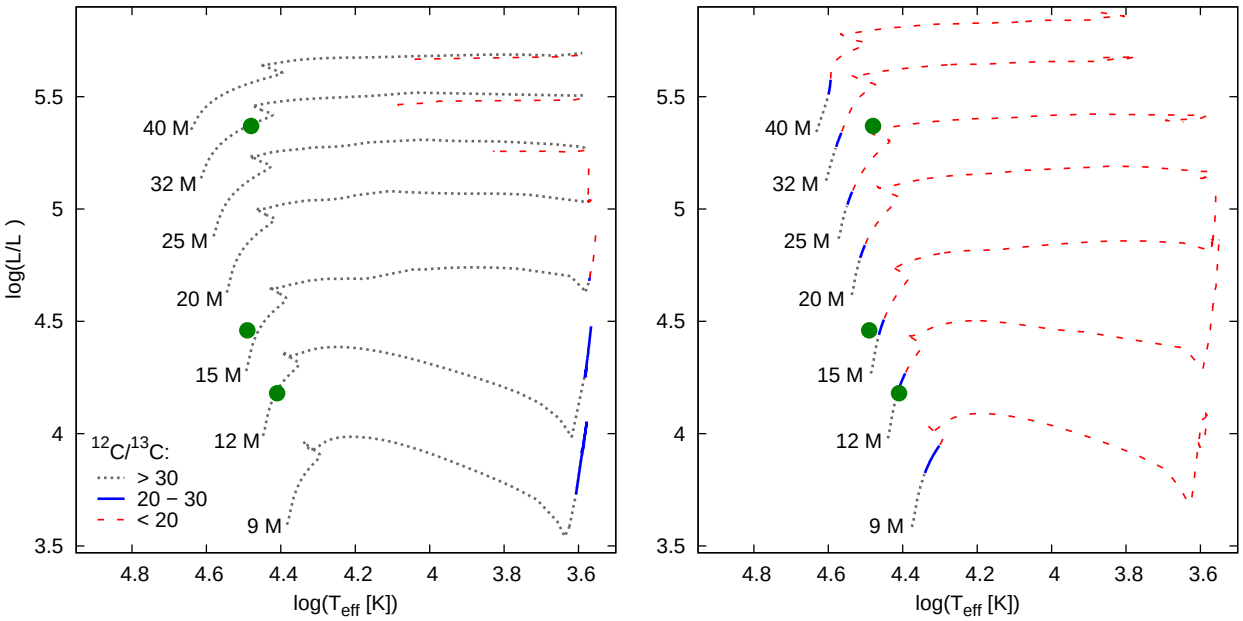

Fig. 5.— HR diagrams showing the location of MWC 137 (green spots) according to the stellar parameters listed in Table 3. The evolutionary tracks from Ekström et al. (2012) for non-rotating (left panel) and rotating (right panel) stars of solar metallicity are also shown. The rotating tracks were computed for an initial rotation rate $v_{\rm ini}/v_{\rm crit} = 0.40$. The change of the ^{12}C/^{13}C ratio during stellar evolution is indicated (dashed line ^{12}C/^{13}C < 20, solid line $20 <$ ^{12}C/^{13}C < 30, dotted line ^{12}C/^{13}C > 30).

ity, projected to the line of sight, of 84 ± 2 km s^{-1}, then the question is how did the disk form if the star was initially rotating very slowly. Although binarity could lead to the formation of a disk, no companion has been detected so far (Baines et al. 2006; Wheelwright et al. 2010). Magnetic fields have also been proposed to cause asymmetries in the ejected material, but to our knowledge no magnetic field measurements exist for MWC 137 to support or deny this possibility. On the other hand, while the shape of the first ^{12}CO band head (blue shoulder and red peak) is typically associated with rotation, it can also result from an equatorial outflow of constant velocity. Hence the kinematics in the CO band emission in MWC 137 could be consistent with the expansion seen in most proto-PNe. Still the question of how the material was confined to the equatorial plane remains.

4.2.2. Main-sequence Star

If the star is still on the main sequence, the surrounding nebula should be composed of swept-up interstellar material, rather than material ejected by the star. The position in the HR diagram consistent with a main-sequence classification is associated with a distance $d = 1.3$ kpc, and since the total size of the nebula in the Hα images is $\sim 1'$, the radius of the structure is ~ 0.2 pc. From the evolutionary tracks of Ekström et al. (2012), we estimate an age of 10 Myr for a 12 M$_\odot$ star, and 7 - 8 Myr for a 15 M$_\odot$ star. According to recent simulations, a star with an initial mass of 15 M$_\odot$ and an age of 7 Myr would have created a bubble with a radius of $\sim$ 10 pc (Georgy et al. 2013), and a similar result is expected for a slightly lower mass star. The size of the nebula around MWC 137 is much too small to be consistent with a scenario of swept-up interstellar material.

The CO band emission originates in a narrow ring, which according to the temperature derived from modeling, is detached from the star but relatively close. One issue with this scenario is the unlikely possibility of early-type main-sequence stars to form and maintain such high-density disks, as strong winds and ionizing radiation make the survival of these structures improbable. The evaporation timescale of pre-main-sequence disks around Herbig Be stars is typically less than 1 Myr (Alonso-Albi et al. 2009). For this reason, disks are usually found around main-sequence stars of later spectral types (A to G). However, Stolte et al. (2010) found a significant number of B-type main-sequence stars with dusty disks in the Arches cluster, and three of these stars even show first overtone CO band emission in their K-band spectra. The cluster has an age of 2.5$\pm$0.5 Myr (Najarro et al. 2004), which is much longer than the evaporation timescale, but still might be compatible with a pre-main-sequence origin of the disks (Olczak et al. 2012). However, given the age range of MWC 137, such an old B-type main-sequence star should definitely have lost its primordial disk.

Further, the presence of chemically enriched material in the ring around MWC 137 is contrary to what is expected from disks around main-sequence stars. The latter should consist of unprocessed matter from the star formation process. Consequently, the material forming the disk around MWC 137 must be of stellar origin. The observed carbon enrichment is consistent with a main-sequence stage of a star with a relatively high initial rotation rate. One of the possibilities for disk formation is related to critical rotation, such as for classical Be stars (e.g. Krtička et al. 2011; Kurfürst & Krtička 2012; Granada et al. 2013). However, the densities in Be star disks are usually not high enough for efficient molecule and dust condensation, excluding MWC 137 as a classical Be star. Therefore, the only mechanism that can result in a high-density chemically enriched disk around an early-B main-sequence star is interaction with a close binary companion, or even full binary merger. Merging of close massive binaries during the main-sequence evolution is predicted by binary evolution models (Sana et al. 2012). A merger scenario could explain the lack of detection of a companion star.

4.2.3. Supergiant

Considering the lower limit of 6 kpc for the distance estimated by Esteban & Fernández (1998), and the corresponding lower limit of $\log(L/L_\odot) = 5.4$ for the luminosity, the value of the ^{12}C/^{13}C ratio derived from the spectral modeling is consistent with a rotating star that has just left the main-sequence and is now entering the supergiant phase. There are two well-known early B-type supergiants in the Galaxy that can be compared to

MWC 137: Sher 25 and SBW1. Their optical images show bipolar lobes and equatorial rings with estimated radii of ~ 0.2 pc (Brandner et al. 1997; Smith et al. 2007). The abundance determinations indicate that these stars did not go through a red supergiant (RSG) phase yet, and that the ring material has most likely been ejected during the blue supergiant (BSG) phase (Hendry et al. 2008; Smith et al. 2007). Hendry et al. (2008) analyze the radial velocity variations of Sher 25 and conclude that it is unlikely that this star has an unseen companion. For SBW1 no evidence of binarity has been reported yet. Instead, it was suggested that the formation of the rings might be connected to rapid rotation of the central stars. The Hα image of MWC 137 shows a structure that could also be interpreted as a bipolar nebula (see Fig. 2 from Marston & McCollum 2008). If the projection of the lobes on the plane of the sky have an apparent size of $\sim 1'$ (see Fig. 3 from Esteban & Fernández 1998), for the distance of 6 kpc the linear radius would be ~ 1 pc.

While on large scales the three objects are comparable, on smaller scales more similarities can be found between SBW1 and MWC 137. The CO emission in MWC 137 must come from a ring close to the star. Nothing is known about molecular band emission from the other BSG, however, Smith et al. (2013) found a narrow and dense torus of warm dust around SBW1. This may suggest that this star could be similar to MWC 137, but in a more evolved stage, in which the initially hot molecular material has expanded, cooled and condensed into dust. This would be compatible with the lack of a dusty disk or ring structure around MWC 137. An additional similarity between these two stars is the fact that in both cases the [O III] emission from the nebula is very weak (Smith et al. 2013).

Since MWC 137 exhibits typical characteristics associated with the B[e] phenomenon, Esteban & Fernández (1998) propose that the star is a B[e] supergiant (B[e]SG). These stars are known to have dense molecular disks or rings, and first overtone CO band emission has been observed in many of them. Detailed modeling of this emission indicates the existence of detached rotating molecular rings with temperatures and column densities comparable to the values derived for MWC 137 around several B[e] supergiants (e.g. Kraus et al. 2010; Liermann et al. 2010; Cidale et al. 2012; Oksala et al. 2013; Kraus et al. 2014). Furthermore, an enhancement of the ^{13}C abundance has been found in these objects, and the values of the carbon isotopic ratio derived by modeling their K-band spectra are, in most cases, consistent with the stars being in a pre-RSG phase (Oksala et al. 2013). Smith et al. (2007) suggest that B[e]SGs could be the progenitors of early BSGs with rings, such as SBW1 and Sher 25. Considering the possibility that MWC 137 is a B[e]SG, its close resemblance to these two early B supergiants might support this idea. However, according to the position in the HR diagram the enrichment in ^{13}C seen in the spectrum is not consistent with a high initial rotation rate, thought to be the mechanism for disk formation in B[e]SGs. Also, as no companion has been detected, the formation of the molecular ring and the large nebular structure remain unclear.

4.2.4. On the Evolutionary Stage of MWC 137

We have presented a brief comparison between MWC 137 and objects in each of the evolutionary phases consistent with the carbon isotopic ratio derived from our data. As was already mentioned, this star shows some characteristics in common with proto-PNe, although the main argument against this classification might be the lack of H_2 emission. However, if MWC 137 were indeed a proto-PN, it would be one of the relatively few B-type stars found in this transition stage, making it an ideal candidate to help identify the characteristics that define these objects and test the stellar evolution theories. Besides, the same unique characteristics that attempt against its classification as proto-PN could help understand the processes involved in the transition from the AGB to the PN phase. The main-sequence classification might be the least likely, given that no compact disks have been confirmed so far around hot main-sequence stars in the age range estimated for MWC 137. The presence of chemically enriched material in the disk of MWC 137 together with the peculiar Hα nebula that surrounds the star complicates the main-sequence picture even more. If MWC 137 were a main-sequence object, a careful study of the mechanisms that led to the origin and characteristics of the circumstellar environment could provide clues to the processes that can

affect mass loss during this phase of the evolution. Given the similarities with other BSGs with bipolar ring nebulae and B[e]SGs stars (e.g., bipolar structure, weak [O III] emission, high-density disk, enhancement of ^{13}C) the supergiant classification seems to be the most plausible. Supporting the supergiant scenario, the profiles of the Pfund lines suggest that they probably originate in a wind or outflow. The presence of a wind is associated with a mass-loss process that could be responsible of the enrichment of the circumstellar medium.

5. CONCLUSIONS

In this paper, we have presented high-resolution K-band spectra of the Galactic B[e] star MWC 137, aimed at studying the molecular component of the circumstellar medium. The low temperature derived by modeling the CO band head features ($T = 1900 \pm 100$ K) indicates that the emitting region is not located in a disk that extends down to the stellar surface, but rather in a narrow, detached ring. This ring seems to be stable, with a rotational velocity, projected to the line of sight, of 84 ± 2 km s^{-1}. The temperature and column density ($N = (3 \pm 1) \times 10^{21}$ cm^{-2}) of the disk resemble those typically found around B[e]SGs.

We also investigate the evolutionary stage of this peculiar object based on the carbon isotopic ratio. The amount of ^{13}CO relative to ^{12}CO in the near-infrared spectrum of MWC 137 is a definite sign of evolution, and confirms that the star cannot be in a pre-main-sequence phase, thus excluding the Herbig Be classification. Considering the classifications reported in the literature and the variation of the ^{12}C/^{13}C ratio along the stellar evolution, we found that the observed isotopic abundance ratio derived from our modeling is compatible with a proto-PN, main-sequence or supergiant evolutionary phase. Furthermore, based on the comparison of observable characteristics of MWC 137 with objects in each of these phases, we propose that the supergiant scenario seems to be the most plausible. Hence, we suggest that MWC 137 could be in an extremely short-lived phase evolving from a B[e] supergiant to a blue supergiant with a bipolar ring nebula.

We thank the referee for the useful comments and suggestions which helped to improve this manuscript. This research has made use of NASA's Astrophysics Data System (ADS), and the SIMBAD database, operated at CDS, Strasbourg, France. M.L.A., L.C. and M.F.M. acknowledge financial support from the Agencia de Promoción Científica y Tecnológica (Préstamo BID PICT 2011/0885), CONICET (PIP 0300), and the Programa de Incentivos (G11/109) of the Universidad Nacional de La Plata, Argentina. M.K. acknowledges financial support from GAČR under grant number 14-21373S. M.E.O. acknowledges the post-doctoral program of the Czech Academy of Sciences. The Astronomical Institute Ondřejov is supported by the project RVO:67985815. Financial support for International Cooperation of the Czech Republic (MŠMT, 7AMB14AR017) and Argentina (Mincyt-Meys, ARC/13/12 and CONICET/14/003) is acknowledged.

REFERENCES

Allen, D. A. 1973, MNRAS, 161, 145

Alonso-Albi, T., Fuente, A., Bachiller, R., et al. 2009, A&A, 497, 117

Amnuel, P. R., Guseinov, O. K., Novruzova, K. I., & Rustamov, I. S. 1984, Ap&SS, 107, 19

Baines, D., Oudmaijer, R. D., Porter, J. M., & Pozzo, M. 2006, MNRAS, 367, 737

Baker, J. G. & Menzel, D. H. 1938, ApJ, 88, 52

Bergner, Y. K., Miroshnichenko, A. S., Yudin, R. V., et al. 1995, A&AS, 112, 221

Berrilli, F., Corciulo, G., Ingrosso, G., et al. 1992, ApJ, 398, 254

Blöcker, T. 1995, A&A, 299, 755

Brand, J. & Wouterloot, J. G. A. 1994, A&AS, 103, 503

Brandner, W., Grebel, E. K., Chu, Y.-H., & Weis, K. 1997, ApJ, 475, L45

Brott, I., de Mink, S. E., Cantiello, M., et al. 2011, A&A, 530, A115

Bujarrabal, V., Alcolea, J., & Neri, R. 1998a, ApJ, 504, 915

Bujarrabal, V., Alcolea, J., Sahai, R., Zamorano, J., & Zijlstra, A. A. 1998b, A&A, 331, 361

Bujarrabal, V. & Alcolea, J. 2013, A&A, 552, A116

Carr, J. S. 1995, Ap&SS, 224, 25

Carr, J. S., Tokunaga, A. T., Najita, J., Shu, F. H., & Glassgold, A. E. 1993, ApJ, 411, L37

Chieffi, A., & Limongi, M. 2013, ApJ, 764, 21

Cidale, L. S., Borges Fernandes, M., Andruchow, I., et al. 2012, A&A, 548, A72

Cohen, M. & Barlow, M. J. 1975, Astrophys. Lett., 16, 165

Ekström, S., Georgy, C., Eggenberger, P., et al. 2012, A&A, 537, A146

Esteban, C. & Fernández, M. 1998, MNRAS, 298, 185

Fich, M. & Blitz, L. 1984, ApJ, 279, 125

Fich, M. & Silkey, M. 1991, ApJ, 366, 107

Finkenzeller, U. & Mundt, R. 1984, A&AS, 55, 109

Frogel, J. A., Persson, S. E., & Kleinmann, D. E. 1972, Astrophys. Lett., 11, 95

García-Hernández, D. A., Manchado, A., García-Lario, P., et al. 2002, A&A, 387, 955

Georgy, C., Walder, R., Folini, D., et al. 2013, A&A, 559, A69

Gledhill, T. M., Forde, K. P., Lowe, K. T. E., & Smith, M. D. 2011, MNRAS, 411, 1453

Gorlova, N., Lobel, A., Burgasser, A. J., et al. 2006, ApJ, 651, 1130

Granada, A., Ekström, S., Georgy, C., et al. 2013, A&A, 553, A25

Hamann, F. & Persson, S. E. 1992, ApJS, 82, 285

Hendry, M. A., Smartt, S. J., Skillman, E. D., et al. 2008, MNRAS, 388, 1127

Herbig, G. H. & Kameswara Rao, N. 1972, ApJ, 174, 401

Hernández, J., Calvet, N., Briceño, C., Hartmann, L., & Berlind, P. 2004, AJ, 127, 1682

Hillenbrand, L. A. 1995, PhD thesis, University of California; Department of Astronomy; 601 Campbell Hall; Berkeley, CA 94720

Hillenbrand, L. A., Strom, S. E., Vrba, F. J., & Keene, J. 1992, ApJ, 397, 613

Hora, J. L., Latter, W. B., & Deutsch, L. K. 1999, ApJS, 124, 195

Hrivnak, B. J., Kwok, S., & Geballe, T. R. 1994, ApJ, 420, 783

Kelly, D. M., & Hrivnak, B. J. 2005, ApJ, 629, 1040

Kraus, M. 2000, PhD thesis, University of Bonn

Kraus, M. 2009, A&A, 494, 253

Kraus, M., Krügel, E., Thum, C., & Geballe, T. R. 2000, A&A, 362, 158

Kraus, M., Borges Fernandes, M., de Araújo, F. X., & Lamers, H. J. G. L. M. 2005, A&A, 441, 289

Kraus, M., Borges Fernandes, M., & de Araújo, F. X. 2010, A&A, 517, A30

Kraus, M., Oksala, M. E., Nickeler, D. H., et al. 2013, A&A, 549, A28

Kraus, M., Cidale, L. S., Arias, M. L., Oksala, M. E., & Borges Fernandes, M. 2014, ApJ, 780, L10

Krtička, J., Owocki, S. P., & Meynet, G. 2011, A&A, 527, A84

Kurfürst, P. & Krtička, J. 2012, in Astronomical Society of the Pacific Conference Series, Vol. 464, Circumstellar Dynamics at High Resolution, ed. A. C. Carciofi & T. Rivinius, 223

Liermann, A., Kraus, M., Schnurr, O., & Fernandes, M. B. 2010, MNRAS, 408, L6

Liermann, A., Schnurr, O., Kraus, M., et al. 2014, MNRAS, 443, 947

Manchado, A., Esteban, C., & Vilchez, J. M. 1989, in Lecture Notes in Physics, Berlin Springer Verlag, Vol. 350, IAU Colloq. 120: Structure and Dynamics of the Interstellar Medium, ed. G. Tenorio-Tagle, M. Moles, & J. Melnick, 129

Marston, A. P. & McCollum, B. 2008, A&A, 477, 193

Martins, F., & Palacios, A. 2013, A&A, 560, A16

McGregor, P. J., Hyland, A. R., & Hillier, D. J. 1988a, ApJ, 324, 1071

McGregor, P. J., Hyland, A. R., & Hillier, D. J. 1988b, ApJ, 334, 639

Miroshnichenko, S. 1994, in Astronomical Society of the Pacific Conference Series, Vol. 62, The Nature and Evolutionary Status of Herbig Ae/Be Stars, ed. P. S. The, M. R. Perez, & E. P. J. van den Heuvel, 134

Morris, P. W., Eenens, P. R. J., Hanson, M. M., Conti, P. S., & Blum, R. D. 1996, ApJ, 470, 597

Muratore, M. F., Kraus, M., Liermann, A., et al. 2010, Boletín de la Asociación Argentina de Astronomía La Plata Argentina, 53, 123

Muratore, M. F., Kraus, M., & de Wit, W. J. 2012, Boletín de la Asociación Argentina de Astronomía La Plata Argentina, 55, 123

Najarro, F., Figer, D. F., Hillier, D. J., & Kudritzki, R. P. 2004, ApJ, 611, L105

Najita, J., Carr, J. S., Glassgold, A. E., Shu, F. H., & Tokunaga, A. T. 1996, ApJ, 462, 919

Oksala, M. E., Kraus, M., Cidale, L. S., Muratore, M. F., & Borges Fernandes, M. 2013, A&A, 558, A17

Olczak, C., Kaczmarek, T., Harfst, S., Pfalzner, S., & Portegies Zwart, S. 2012, ApJ, 756, 123

Oudmaijer, R. D., Waters, L. B. F. M., van der Veen, W. E. C. J., & Geballe, T. R. 1995, A&A, 299, 69

Paczyński, B. 1970, Acta Astron., 20, 47

Paczyński, B. 1971, Acta Astron., 21, 417

Perek, L. & Kohoutek, L. 1967, in Acad. Publ. House of the Czech. Acad. Sci., 1-276 (1967), 1–276

Rudolph, A. L., Brand, J., de Geus, E. J., & Wouterloot, J. G. A. 1996, ApJ, 458, 653

Sabbadin, F. & Hamzaoglu, E. 1981, A&A, 94, 25

Sana, H., de Mink, S. E., de Koter, A., et al. 2012, Science, 337, 444

Sharpless, S. 1959, ApJS, 4, 257

Smith, N., Arnett, W. D., Bally, J., Ginsburg, A., & Filippenko, A. V. 2013, MNRAS, 429, 1324

Smith, N., Bally, J., & Walawender, J. 2007, AJ, 134, 846

Stolte, A., Morris, M. R., Ghez, A. M., et al. 2010, ApJ, 718, 810

Testi, L., Palla, F., & Natta, A. 1998, A&AS, 133, 81

Thé, P. S., de Winter, D., & Pérez, M. R. 1994, A&AS, 104, 315

Vassiliadis, E. & Wood, P. R. 1994, ApJS, 92, 125

Verhoeff, A. P., Waters, L. B. F. M., van den Ancker, M. E., et al. 2012, A&A, 538, A101

Wheelwright, H. E., Oudmaijer, R. D., & Goodwin, S. P. 2010, MNRAS, 401, 1199

Wouterloot, J. G. A., Brand, J., & Henkel, C. 1988, A&A, 191, 323

Zhang, C. Y. 1995, ApJS, 98, 659

Zickgraf, F.-J. 2003, A&A, 408, 257

This 2-column preprint was prepared with the AAS LaTeX macros v5.2.

Table 3: Stellar parameters for MWC 137 taken from the literature.

$\log T_{\rm eff}$ (K)	$\log L$ ($L_\odot$)	Ref.	Classification [a]	d (kpc)
4.41	4.18	1	PMS / MS	1.3
4.49	4.46±0.04 [b]	2	PMS / MS	1.3
4.48	5.37 [c]	3	SG	6 [c]

[a] PMS = pre-main-sequence; MS = main-sequence; SG = supergiant.

[b] Values in the references range from 4.42 to 4.5.

[c] Lower limit according to Esteban & Fernández (1998).

References. — (1) Alonso-Albi et al. (2009); (2) Hillenbrand et al. (1992); Hillenbrand (1995); Testi et al. (1998); Verhoeff et al. (2012); (3) Esteban & Fernández (1998).